

UCSF

UC San Francisco Previously Published Works

Title

Quantitatively Characterizing Drug-Induced Arrhythmic Contractile Motions of Human Stem Cell-Derived Cardiomyocytes

Permalink

<https://escholarship.org/uc/item/0qz9n9pt>

Authors

Hoang, Plansky
Huebsch, Nathaniel
Bang, Shin Hyuk
et al.

Publication Date

2018-04-12

DOI

10.1002/bit.26609

Peer reviewed

Quantitatively Characterizing Drug-Induced Arrhythmic Contractile Motions of Human Stem Cell-Derived Cardiomyocytes[†]

Plansky Hoang,^{1,2} Nathaniel Huebsch,^{3,4} Shin Hyuk Bang,¹ Brian A. Siemons,³

Bruce R. Conklin,^{5,6} Kevin E. Healy,^{3,4} Zhen Ma,^{1,2,*} Sabir Jacquir,^{7,*}

¹Department of Biomedical & Chemical Engineering, Syracuse University, Syracuse, NY, USA

²Syracuse Biomaterials Institute, Syracuse University, NY, USA

³Department of Bioengineering, University of California, Berkeley, CA, USA

⁴Department of Material Science & Engineering, University of California, Berkeley, CA, USA

⁵Glastone Institute of Cardiovascular Diseases, San Francisco, CA, USA

⁶Department of Medicine, and Cellular and Molecular Pharmacology, University of California, San Francisco, CA, USA

⁷Laboratoire LE2I UMR CNRS 6306, Université de Bourgogne Franche-Comté, Dijon, France

*Correspondence: Sabir Jacquir (sjacquir@u-bourgogne.fr) and Zhen Ma (zma112@syr.edu)

[†]This article has been accepted for publication and undergone full peer review but has not been through the copyediting, typesetting, pagination and proofreading process, which may lead to differences between this version and the Version of Record. Please cite this article as doi: [10.1002/bit.26709]

Additional Supporting Information may be found in the online version of this article.

This article is protected by copyright. All rights reserved

Received October 26, 2017; Revision Received March 7, 2018; Accepted April 6, 2018

This article is protected by copyright. All rights reserved

ABSTRACT

Quantification of abnormal contractile motions of cardiac tissue has been a noteworthy challenge and significant limitation in assessing and classifying the drug-induced arrhythmias (i.e. Torsades de pointes). To overcome these challenges, researchers have taken advantage of computational image processing tools to measure contractile motion from cardiomyocytes derived from human induced pluripotent stem cells (hiPSC-CMs). However, the amplitude and frequency analysis of contractile motion waveforms doesn't produce sufficient information to objectively classify the degree of variations between two or more sets of cardiac contractile motions. In this paper, we generated contractile motion data from beating hiPSC-CMs using motion tracking software based on optical flow analysis, and then implemented a computational algorithm, phase space reconstruction (PSR), to derive parameters (embedding, regularity, and fractal dimensions) to further characterize the dynamic nature of the cardiac contractile motions. Application of drugs known to cause cardiac arrhythmia induced significant changes to these resultant dimensional parameters calculated from PSR analysis. Integrating this new computational algorithm with the existing analytical toolbox of cardiac contractile motions will allow us to expand current assessments of cardiac tissue physiology into an automated, high-throughput, and quantifiable manner which will allow more objective assessments of drug-induced proarrhythmias. This article is protected by copyright. All rights reserved

Keywords: Optical Flow, Biosignal processing, Cardiac Motion, Arrhythmia, Phase space reconstruction

INTRODUCTION

Drug-induced cardiac toxicity is one of the primary reasons for the failures of drug development pipeline and even post-clinical removal due to cardiac side effects after reaching the market (Liang et al., 2013). Recent advances in human induced pluripotent stem cell (**hiPSC**) technology have offered new insights into modeling cardiac tissue *in vitro* and screening drug-induced cardiotoxicity. Neonatal rat cardiomyocytes (**nrCMs**) are used as viable drug-screening platforms, but species differences present challenges in fully recapitulating human physiology and drug response (Sinnecker, Laugwitz, & Moretti, 2014). It has been shown that beat rhythm was more stable in hiPSC-derived cardiomyocytes (**hiPSC-CMs**) compared to nrCMs, as well as high drug sensitivity and responsiveness of hiPS-CMs (Yu et al., 2016). Treatment of hiPSC-CMs with norepinephrine and isoproterenol produced changes in beat rate and contractility that was consistent with adult human heart slices, further suggesting the potential of hiPSC-CMs in screening for drug-induced cardiotoxicity (Navarrete et al., 2013). With the development of heart-on-chip technologies, pharmacological studies on the cardiac microphysiological system showed that IC50 and EC50 values were more consistent with the data from tissue-scale references compared to cellular-scale studies (Mathur et al., 2015).

Cardiac drug responses are often characterized as changes in heart rate, contractility and rhythm. Therefore, evaluation of the cardiac contraction is a wide-accepted means for determining the pathophysiological status of hiPSC-CMs. Quantitative methods for cardiac contraction analysis based on computational image processing, such as pixel intensity monitoring (Hossain et al., 2010) and edge detection (Bazan, Torres Barba, Blomgren, & Paolini, 2011), have been applied to minimize judgment variations, but these methods are limited by introducing user-dependent bias on defining contours and segmenting the cells during image processing. To overcome these barriers, automated optical flow analysis based on block matching algorithms offered a more robust alternative to detect cardiac contractile

motion (Duan, Angelini, & Gerard, 2006; Hassanein, Khalifa, Al-Atabany, & El-Wakad, 2014; Huebsch et al., 2015; Lee, Kurokawa, Tu, George, & Khine, 2015; Maddah et al., 2015; Torkashvand, Behnam, & Sani, 2012). By tracking the position of blocks of pixels frame by frame within a video, we were able to generate motion vectors to estimate the hiPSC-CMs contractility.

Standard and well-established technologies to assess drug-induced arrhythmia of hiPSC-CMs include microelectrode arrays (MEAs) (Kempf et al., 2014; X. Q. Xu, Soo, Sun, & Zweigerdt, 2009) and patch clamp analysis. Optical flow analysis of hiPSC-CMs contractile motion granted many advantages over these traditional electrophysiological approaches. It provides the possibility to evaluate the contractile functions at a variety of spatial scales from single cells to 3D cardiac tissues. Furthermore, this video-based method offered non-invasive measurements, thus cell and tissue culturing environments remained undisturbed for long-term monitoring. However, current optical flow analysis suffers from simplified conventional analytical tools of dominant frequency analysis (Narayan et al., 2011) and amplitude analysis (Wood, Moskovljevic, Stambler, & Ellenbogen, 1996), providing time-series waveforms with measurement of beat rate, contraction velocity, relaxation velocity and beat duration. Such analysis cannot faithfully predict the complex biological behaviors and physiological signals to determine and classify the level of arrhythmic contraction response to drug interference quantitatively, statistically and systematically.

To address this limitation, we took advantage of mathematical chaos theory to identify the nonlinear dynamic characteristics of hiPSC-CMs contractile motions recorded using optical flow and block-matching methods. More specifically, a phase space reconstruction (**PSR**) method (Brzozowska & Borowska, 2016; Huffaker, 1997; Kliková & Raidl, 2011; Richter & Schreiber, 1998) was used to convert our biological dynamic system into a phase space consisting of a set of typical trajectories, in which each point is corresponding to a system state. PSR has previously been applied to analyze electrophysiological

signals to identify arrhythmia both *in vitro* and *in vivo*. Electrical field potentials from nrCMs recorded by MEA were subjected to PSR to compute the parameters that quantified the unique dynamics of normal versus arrhythmic signals (B. Xu, Jacquir, Laurent, Bilbault, & Binczak, 2014). PSR was also used to analyze heart rate intervals of electrocardiograms (ECGs) (Mironyuk & Loskutov, 2006; Richter & Schreiber, 1998) and magnetic resonance image (MRI) data (Cîndea, Odille, Bosser, Felblinger, & Vuissoz, 2010) acquired from patients with different heart pathologies. The parameters computed from PSR, such as embedding and correlation dimensions, varied considerably between groups with different heart diseases, further reiterating the ability of PSR to quantitatively measure the dynamics of cardiac signals (Mironyuk & Loskutov, 2006).

In this study, we developed a computational algorithm based on PSR to depict the deterministic dynamics of chaotic nature in the contractile motions of cardiac tissues before and after drug administration. Through PSR, one-dimensional (1D) time-series signals can be mathematically modeled in high-dimensional space to derive parameters for signal characterization. The new algorithm provided us an analytical tool to quantitatively classify the arrhythmic contractile motions of hiPSC-CMs for more precise drug cardiotoxicity screening workflow. By integrating hiPSC technology, optical flow computation and this new analytical tool, we envisage to measure abnormalities in heart contraction related to drug-induced arrhythmia in an automated, high-throughput and quantifiable manner.

RESULTS and DISCUSSION

Reconstruction of time-series contraction waveform

First, we determined the capability of PSRs to reflect the dynamics of cardiac contractile motion of hiPSC-CMs. The hiPSC-CMs differentiated in our studies positively expressed cardiac-specific markers, including cardiac troponin T, cardiac troponin I, β myosin heavy chain, sarcomeric α -actinin,

connexin 43, desmoplakin and N-cadherin (Figure S1a-f). Flow cytometry analysis showed that we were able to achieve consistent differentiation efficiency of over 65% (Fig. S1g). The workflow of our analytical approach started with video recording of beating hiPSC-CMs, plated in standard 2D culture, using a bright-field or phase contrast microscope. The recorded videos were subjected to motion tracking analysis to generate motion vectors that measure the motion velocity and beat frequency. Motion tracking data was then decomposed using PSR and from this, a set of dimensional parameters can be generated to reflect the dynamics of the motions regarding to regularity and complexity (Fig.1). We then selected two motion waveforms generated from video analysis using motion tracking software, one represented regular cardiac contraction (Movie S1), while the other represented irregular (complex) cardiac contraction (Movie S2). Then, we reconstructed these two motion waveforms into phase space respectively. For each time lag, we can reconstruct a corresponding phase space through the time lagged method (Fig. S2a, b), and the PSR evolved with the increase of time lag for each motion waveform (Movie S3 & S4). We selected the PSR with $\tau = 15$ for both motion waveforms and showed that the PSR for complex contractile motion appeared to have higher degrees of convolution and eccentricity in comparison to the PSR for regular motion (Fig. 2a-d). This verified that distinct cardiac motion waveforms can be represented in the phase spaces that were spatially distinguishable from one another.

Output parameters from the PSRs include the embedding (m), regularity ($\rho = \frac{\tau}{m}$) and fractal (d) dimensions. The embedding and regularity dimensions measure the overall rhythmic regularity of the gross peaks within a waveform, while fractal dimension quantifies the complexity, which is a measure of the aberrations within the system (Fig. 1). We compared embedding dimension for the single waveforms of both regular and complex motion by averaging all values over the entire variance of time lag. The average embedding dimension for complex cardiac contractile motion was significantly greater than the average for regular motion (Fig. 2e), which translated to lower regularity dimensions over all values of

time lags (Fig 2f). We can utilize embedding and regularity dimensions to measure and compare the motion regularity between two distinct waveforms. In contrast, the fractal dimension quantifies the complexity of the waveforms. We found that the fractal dimension was greater for complex contractile motion, which was consistent for all the time lags (Fig. 2g, h), inferring that larger values of fractal dimension reflect greater complexity of the time series.

Contraction motion decomposition

Next, we evaluated the PSRs ability to measure the differences in the dynamics of a motion waveform decomposed into its' X and Y directions. We obtained the X and Y components of a cardiac contractile motion waveform from the motion tracking software and treated them as individual waveforms compared against the total motion (Fig. 3a). We then reconstructed the X, Y, and total motion waveforms into their corresponding phase spaces (Fig. 3b), plotted the embedding, regularity and fractal dimensions, and further quantified the regularity and complexity of the cardiac contractile motion (Fig. 3c-f).

The average embedding and regularity dimensions were consistent between the total motion and the corresponding motion along the X and Y directions (Fig. 3c&d), implying that regularity of cardiac contractile motion is independent from the motion along a specific direction. Although the waveforms appear different, the beat rhythm remains conserved, since decomposing the waveform into different directions doesn't influence the overall rhythmic regularity and beat rate. However, the fractal dimension, indicating the motion complexity, was greater for total and X-axis motion in comparison to Y-axis motion for all time lags greater than ~15 (Fig. 3f). The average fractal dimensions for the total and X-axis motion were comparable, but slightly greater than the one for Y-axis motion (Fig. 3e). Thus, Y-axis motion was generally less complex for this particular waveform, which can be visualized in the Y-axis motion

waveform with less distinct peaks for each beat (Fig. 3a). This illustrates that the complexity of motion along an axis varies and that these differences are quantifiable from the parameters derived from PSR.

Noise Sensitivity of PSR

To further characterize the different dimension parameters responding to the system aberrations, we then applied random background noise ranging from 0-50% of the mean contraction velocity to a signal. The addition of background noise generated random deviations within the original motion waveforms, allowing us to study the influence of noise on the regularity and complexity of the cardiac contractile motion. By visual inspection, the increasing increments of noise introduced coarser aberrations within the signal, but the overall rhythmic regularity remained constant, as indicated by the identical gross contraction peaks (Fig. 4a). The addition of random noise, therefore, didn't influence the regularity of the motion, since the overall cardiac beating rhythm wasn't altered. Thus, the embedding and regularity dimensions remained constant for all quantities of random noise (Fig. 4b, c). Since noise creates variations in the signal, we found that increasing levels of noise on the original signal led to an increase of fractal dimensions (Fig. 4d, e), which suggested that the fractal dimension is sensitive to noise and secondary variations in the signal. Therefore, we can quantify the secondary aberrations as the system complexity for the cardiac contractile motion.

Drug response

We first evaluated the experimental heterogeneity of hiPSC-CMs in order to determine how the differentiation variation can impact this analytical approach on drug responses. The batch-to-batch heterogeneity of hiPSC-CMs was characterized using the motion tracking and PSR analytical approach (Fig. S3). We found no significant difference on both contraction velocity and beat rate among different

batches of hiPSC-CM differentiation (Fig. S3a). From PSR analysis, we demonstrated that the dimensional parameters were also negligibly affected by independent repeats hiPSC-CM differentiation, as indicated by relatively constant embedding and fractal dimensions across different hiPSC passage numbers (Fig. S3b). This means that the regularity and complexity of the contractile physiology is not likely a result of inter-experimental heterogeneity. Therefore, subsequent arrhythmia-like responses were attributed to the drug supplements.

To investigate the ability of PSR method for quantifying the drug-induced cardiac motion abnormalities, indicative of cardiac arrhythmia, we treated hiPSC-CMs with four drugs (propranolol, E4031, metoprolol, and isoproterenol) known to influence cardiac beat rhythm and motion. For each drug, we first recorded the beating videos of baseline control, then treated the hiPSC-CMs with two different drug concentrations, and generated corresponding motion waveforms using motion tracking software (Fig. S4a-d). By performing motion tracking analysis on the beating videos, we analyzed the beat rate and maximum contractile velocity (MCV) of the hiPSC-CMs treated with different drug concentrations versus the baseline control. The beat rate was defined as beats per minute based on frequency analysis of the motion waveforms, while the MCV was defined as the average contraction peak magnitude based on amplitude analysis of the motion waveforms. Next, we performed the PSR analysis on the motion waveforms and computed the corresponding embedding, regularity and fractal dimensions.

Propranolol, a beta blocker used to treat high blood pressure and post-myocardial infarction, has been reported to induce arrhythmias by causing bradycardia. We observed abrupt arrhythmic motion, indicated by the boxed regions of the motion waveforms, as a result of propranolol treatment (Fig. S4a). We also observed significant decreases in beat rate and MCV with increasing concentrations of propranolol (Fig. S5a). The resulting PSR analyses showed that, with respect to propranolol (Fig. 5a), the average embedding dimension increased with increasing propranolol concentration, which translated to a

reduction of regularity dimension with higher concentrations of propranolol. However, fractal dimensions have no significant difference between baseline and two concentrations of propranolol, indicating propranolol treatment did not dramatically influence the complexity of cardiac contractile motions.

E4031 is a hERG potassium ion channel blocker that prolongs the QT interval and result in lethal arrhythmias. Application of E4031 to hiPSC-CMs decreased beat rate and MCV (Fig. S5b). Treatment with E4031 (Fig. 5b), displayed increased embedding dimension and decreased regularity dimension in response to the drug, which implied that E4031 induced arrhythmic contractile motions. Furthermore, E4031 treatment induced an increase of fractal dimension, especially for high dosage of the drug. This suggested that E4031 not only induced arrhythmic motions, but also induced contractile aberrations to the hiPSC-CMs.

Metoprolol is a beta blocker and is used to treat conditions that cause abnormally fast heart rate. Metoprolol-induced arrhythmias (bradycardia) can occur at excessive dosages. Application of metoprolol up to 40 μ M resulted in no significant changes of contraction motion (Fig. S5c). Although metoprolol falls within the same drug category as propranolol, it is a milder and less potent beta-adrenoceptor antagonist with lower effect of attenuating beat rate than propranolol(Ahokas, Davies, & Ravenscroft, 1984; Sklar et al., 1982). Based on the PSR analysis, there was no significant difference in either the embedding, regularity, or fractal dimensions for all concentrations of the drug (Fig. 5c). This indicated that metoprolol does not induce arrhythmic contractile motion on hiPSC-CMs based on PSR analysis, as this drug does not significantly affect the regularity and the complexity of the system.

Lastly, isoproterenol is a beta adrenoceptor agonist that treats bradycardia. This drug can accelerate the heart rate and potentially induce tachycardia. Application of isoproterenol not only increased both beat rate and MCV (Fig. S5d), but also significantly changed the embedding and fractal dimensions with increasing concentration of drug (Fig. 5d). In particular, the embedding dimension significantly decreased

from the baseline control to a low dosage (50 nM) of isoproterenol. However, as the drug concentration increased further to 10 μ M, the embedding dimension increased. This suggested that low concentrations of isoproterenol had the therapeutic effect of rescuing arrhythmic contractile motions to more regular and consistent motions. However, overdose of isoproterenol might cause the heart beating to lose its' regular rhythm. The average fractal dimension increased with isoproterenol treatment, indicating that the contractile motion became more complex, partially due to the increase of beat rate.

By analyzing the contractile motions of hiPSC-CMs exposed to these four drugs at different concentrations, we found that frequency analysis (beat rate) and amplitude analysis (MCV) could only prove the functionality of specific drug. For example, isoproterenol supposedly increased the beat rate and MCV, while E4031 decreased both parameters (Fig. S5). The risk level of drug-induced arrhythmic motion was not well characterized solely relying on this analysis. However, by performing PSR analysis on these waveforms, we were able to characterize the system dynamics of the hiPSC-CMs contractile motion, and further compute their regularity and complexity as quantifications of drug risk level (Fig. 5). For example, exposure of E4031 at low dosage would potentially induce arrhythmic contractile motion, while low dosages of isoproterenol could help regulate the heart rhythm and diminish the arrhythmia.

Comparison with calcium flux assay

Using GCaMP6f hiPSC-CMs, we validated the performance of our new PSR algorithm on both optical flow motion analysis and calcium flux analysis, one of the standard assays of cardiac electrophysiology. GCaMP6f hiPSC line has been generated to visualize the calcium flux on the living hiPSC-CMs without any fluorescent markers (Movie S5) (Huebsch et al., 2016). PSR analysis is not only limited to the waveforms generated from the contractile motion tracking based on the optical flow method. This analytical algorithm can be also used to analyze the waveforms of electrophysiological signals

generated across a wide range of standard assays. By applying isoproterenol and propranolol to GCaMP6f hiPSC-CMs, we generated the corresponding waveforms from motion tracking analysis and the transient calcium flux (Fig. 6a-c). We performed the PSR analysis on both contractile motion data and calcium flux data to determine the arrhythmic-like behaviors responding to different drug interference.

Based on the PSR analysis coupled with optical flow motion tracking, GCaMP6f hiPSC-CMs treated with isoproterenol showed an improvement in regularity (low embedding dimension and high regularity dimension) at a 10 nM drug concentration (Fig. 6d). This trend was validated in the PSR analysis coupled with the calcium flux measurement, where we also observed low embedding dimensions and higher regularity upon exposure to the drug. This indicated that both approaches are sensitive to changes in the regularity of the system. We also observed increased fractal dimensions in response to 10 nM isoproterenol treatment from PSR coupled with motion tracking. However, this did not match with the calcium flux analysis, where we observed an overall fractal dimension decrease, indicating that physical contractions and electrophysiology represent different complexities in the cardiac physiology. By treating GCaMP6f hiPSC-CMs with propranolol at 10 μ M (Fig. 6e), we observed a significant increase in the embedding dimensions from the PSR algorithm coupled with both motion tracking and calcium flux. We also found a significant increase of fractal dimensions with the 10 μ M propranolol addition from the PSR analysis of both assays. Thus, both assays coupled with PSR showed that treatment of propranolol reduced the regularity and subsequently enhanced the complexity of the cardiac physiology. These results indicated that electrophysiological assays coupled with PSR analysis not only validated our optical flow method, but also served as complimentary assessment for future multiplexed drug-induced arrhythmia analysis.

We have determined that PSR analysis can be applied to two different approaches (contractile motion tracking and calcium flux measurement) for *in vitro* assessments of hiPSC-CM arrhythmic

potential. To further compare the sensitivities of each assay to the drug interference when coupled with PSR algorithm, we performed statistical analyses (*t*-tests) on the PSR outputs (embedding and fractal dimensions) for the drug-treated hiPSC-CMs relative to baseline controls. We then cross-examined the *p*-values of the PSR data generated from motion tracking with those generated from calcium flux measurement. For GCaMP6 hiPSC-CMs treated with isoproterenol, the *p*-values computed from the embedding dimensions was less for motion tracking, compared to the calcium flux ($p<0.0001$ vs. $p=0.0003$). This was also consistent with the embedding dimensions calculated from propranolol treatment, where the *p*-values were $p<0.0001$ and $p=0.0276$ for motion tracking and calcium flux, respectively. For isoproterenol treated hiPSC-CMs, the *p*-value of the fractal dimensions was found to be larger for motion tracking ($p=0.01$) compared to the calcium flux ($p<0.0001$). From the propranolol treatment, the *p*-values of fractal dimensions between the motion tracking and calcium flux were comparable ($p<0.0001$).

The smaller *p*-values calculated from the embedding dimensions coupled with motion tracking, a consistent trend between both drugs, indicated that the PSR regularity quantification is more sensitive to the physical contraction recorded using the motion tracking approach. *P*-values from analysis of the fractal dimension were found to be comparable between the motion tracking and the calcium flux assays of propranolol treatment. This suggests that the quantification of system complexity is equally sensitive to both assays. However, this was not consistent with isoproterenol treatment, where complexity computation was found to be more sensitive to the calcium flux (as indicated by the smaller *p*-value). This inconsistency was attributed to our previous observation, where the electrophysiology and the physical contraction represented different system complexities.

CONCLUSIONS

A combination of optical flow-based motion tracking and PSR analysis was used to characterize and quantify the arrhythmic behavior of cardiac contractile motion. In this paper, we reconstructed 1D time series of contractile motion waveforms obtained from optical flow analysis of hiPSC-CMs into a multi-dimensional phase space, and then distinguish the different biological dynamics based on the embedding, regularity and fractal dimensions. Based on PSR analysis, we evaluated the drug-induced arrhythmic contractile motion from hiPSC-CMs and concluded that the regularity and complexity of cardiac contractile motion changes in response to the drugs. We have also shown that PSR is not limited to the reconstruction of motion waveforms, as it can also be applied to time series waveforms derived from other standard assays of cardiac physiology and arrhythmic potential. By integration with machine learning to optimize predictions of cardiotoxicity at a larger scale, we envisage that this computational algorithm can be applied to classify the cardiotoxicity of newly developed drugs, and potentially establish a new full-automated, low-cost, high-throughput analytical toolbox for human-specific drug screening purpose.

MATERIALS and METHODS

hiPSC culture and differentiation

Wild-type (WT) hiPSCs were reprogrammed from dermal fibroblasts obtained from a healthy volunteer with no prior family history of cardiac disease. hiPSCs were maintained and passaged at least three times with Essential 8 medium (Life Technologies) at a constant density of 8000 cells/cm² on growth factor-reduced Matrigel (BD Biosciences) coated substrates. Cardiac differentiation was performed via modulation of the canonical Wnt signaling pathway (Lian et al., 2012). hiPSCs were first seeded onto Matrigel-coated -6-well tissue culture plates at 25,000 cells/cm² in E8 media supplemented with 10 μ M

Y-27632 (Sigma). After 24 h, the medium was exchanged to E8 without Y-27632, and the cells were expanded for an additional 48 hours by daily media changes. On day 0, hiPSCs were treated with 12 μ M of the GSK3-b inhibitor, CHIR99021 (CHIR; Tocris), in RPMI 1640 medium containing B27 supplement minus insulin (RPMI/B27-I; Life Technologies). Twenty-four hours after CHIR treatment (day 1), the medium was switched to RPMI/B27-I and cells were left undisturbed for an additional 48 h. On day 3, cells were exposed to a 50:50 mixture of conditioned media and fresh RPMI/B27-I, supplemented with 5 μ M Wnt inhibitor, IWP-2 (Tocris). Two days (48 h) later, the media was changed to RPMI/B27-I for 2 days, and afterward changed to RPMI 1640 containing B27 complete supplement (RPMI/B27C; Life Technologies) on day 7. This completed the cardiac differentiation procedure and RPMI/B27C medium was changed thereon out every three days. For analysis and quantification, we excluded singular, isolated regions of beating tissue because these regions are typically surrounded by static tissue that can interfere with the contraction. Therefore, regions of differentiated tissue exhibiting visibly beating sheets were used for motion tracking analysis. We characterized sheets of cardiac tissue as monolayers of tissue that exhibit uniform, wave-like beating.

Video microscopy and motion tracking analysis of hiPSC-CMs

hiPSC-CMs were imaged in an onstage microscope incubator at 37 °C and 5% CO₂ to maintain standard physiological conditions on a Nikon Eclipse TS100F microscope with Hamamatsu ORCA-Flash4.0 V2 digital CMOS camera. Video recordings of the beating hiPSC-CMs were taken at 100 fps over 10 s in brightfield and exported as a series of single-frame image files. Motion tracking analysis was performed by importing the video recordings into our open source and in-house developed software capable of generating waveforms of the contractile motion(Huebsch et al., 2015). The software takes advantage of optical flow and block matching to calculate motion vectors by tracking the movement of

macroblocks of pixels from one frame to another. To evaluate hiPSC-CMs response to drugs, media was supplemented with the addition of 10X stock solutions. Immediately following the baseline imaging, media containing the drug was rapidly added to the hiPSC-CM samples. Motion tracking of hiPSC-CMs was performed using the same procedure described above and compared to baseline contraction.

Calcium flux imaging and analysis of GCaMP6f hiPSC-CMs

For calcium flux imaging, GCaMP6f hiPSC-CMs were generated from GCaMP6f hiPSC line with the same differentiation protocol. GCaMP6f hiPSC-CMs can activate the fluorescence from green fluorescent protein as an indication of the increased cytoplasmic calcium levels that occur during hiPSC-CM contraction. The calcium flux images were recorded at 30 frames per second for 10 seconds and exported as single frame images. The fluctuations in fluorescent intensity were plotted by the Z-axis profile in ImageJ, corrected the fluorescent bleaching decay by in-house MATLAB script, and analyzed by phase space reconstruction algorithm. For drug response studies, we recorded the baseline contraction in both brightfield transmitting light for motion analysis and the fluorescence emitted by the GCaMP protein for calcium flux analysis. Each drug was incrementally added to the culture media to achieve a range of treatment concentrations and videos were recorded immediately after each addition.

Phase space reconstruction

The principle of this approach is to transform the properties of a time series into topological properties of a geometrical object embedded in a space, in which all possible states of the system are represented and each state corresponds to a unique vector (Gao & Jin, 2009). Mathematically, the states of a m dimensional dynamic system can only be characterized by m independent quantities that represent the coordinates of the phase space. Unfortunately, this representation is not possible for experimental data,

because it is a 1D time series. Starting on the conjecture that all groups of m values should give equivalent results, it is then possible to construct m -vectors that contain the same information as the original state vectors: this is the principle of the time lagged method (Takens, 1981), which simply takes m consecutive elements of the time series directly as coordinates in the phase space. The challenge is to find the appropriate number m , such that the properties of the initial time series are kept in the reconstructed space. A method consisting of building a m dimensional system from a 1D time series with a fixed delay to shift the original data (time lagged method) has been introduced by Takens (Takens, 1981).

Let be the system states with a normalized sample step $T = 1$, $\tau \in \mathbb{N}^*$, while $i = 1, 2, \dots, n$ are the indices of the successive samples values of the cardiac contraction motion waveform s :

$$V(\tau, m) = [\vec{S}(i), \vec{S}(i + \tau), \dots, \vec{S}(i + (m - 1)\tau)], \quad (1)$$

where V is a matrix containing the phase space vectors:

$$V(\tau, m) = \begin{bmatrix} s(1) & s(2) & \dots & s(N - (m - 1)\tau) \\ s(1 + \tau) & s(2 + \tau) & \dots & s(N - (m - 2)\tau) \\ \cdot & \cdot & \dots & \cdot \\ \cdot & \cdot & \dots & \cdot \\ \cdot & \cdot & \dots & \cdot \\ s(1 + (m - 1)\tau) & s(2 + (m - 1)\tau) & \dots & s(N) \end{bmatrix} \quad (2)$$

Next, Takens theorem (Takens, 1981) gives conditions under which a nonlinear dynamical system can be reconstructed from a sequence of observation of its states. A schematic illustration of the state space reconstruction of a system from one sample signal is depicted in Supplemental Figure 1. The state

space vectors are obtained from the sample signal according to the embedding dimension m and the time delay τ . The embedding dimension m is computed for each time delay τ based on False Nearest Neighbor (FNN) method, and resulting phase space vectors obtained from (1) are:

$$V(1, 3) = [\vec{S}(i), \vec{S}(i + 1), \vec{S}(i + 2)], \quad (3)$$

$$V(3, 3) = [\vec{S}(i), \vec{S}(i + 3), \vec{S}(i + 6)], \quad (4)$$

$$V(6, 3) = [\vec{S}(i), \vec{S}(i + 6), \vec{S}(i + 12)], \quad (5)$$

$$V(9, 2) = [\vec{S}(i), \vec{S}(i + 9)], \quad (6)$$

The phase space reconstruction is influenced by the parameter time lag τ . If τ is too small, the trajectories of $\vec{S}(i)$ and $\vec{S}(i + \tau)$ are close to one another, potentially making it indistinguishable and creating redundant coordinates. This implies that the trajectories of attractor projected on the two axes are not correlated, which makes the phase space reconstruction useless. For this reason, the basic criterion for choosing τ should be the largest value of τ resulting coordinates relatively independent. Without prior knowledge of the system, especially for experimental data, properly determining this parameter is not apparent. Therefore, in this study, for cardiac contraction motion waveforms, the time lag τ has been varied from $\tau = 1 - 50$.

To estimate the embedding dimension m , we used FNN method, where the best value of m corresponds to the minimum value of m for which the FNN is close to zero (Krakovská, Mezeiová, & I, 2015). From a geometrical point of view, the time series (experimental measurements) is the projection of a m dimensional system to a 1D space. Therefore, two points in a m dimensional space, even far from each other, could be very close (and even be superimposed) in the original 1D space. These points are called *false neighbors*. If m is not large enough, the state vectors on the trajectories could be very close with possibility of intersections between the trajectories of the attractor, which will result in a

reconstructed space totally different from the original one. A higher value of m , theoretically, is possible by just creating a larger space that contains minimal space. However, this will cause redundant problems and inefficiency issue, as it requires significantly strong computation power. The main idea behind this method is to determine an appropriate value of m as follows:

- We begin the reconstruction with vectors of delay $\vec{S}(i)$ of dimension m small enough;
- We determine the neighbors of each $\vec{S}(i)$ by checking $\|\vec{S}(j) - \vec{S}(i)\| \leq \varepsilon$, where ε is a length appropriate to the problem and containing the number of these neighbors;
- We increase m until the neighbor numbers stabilize.

To quantify the regularity of the time series of cardiac contraction waveform, we introduce a new parameter called “Regularity Dimension” noted as ρ , which is defined as:

$$\rho = \frac{\tau}{m} \quad (7)$$

To quantify the complexity of time series of cardiac contraction waveform, we compute the fractal dimension d using Boxcount method and Variation estimator. In the case of Boxcount method, it is supposed that the original time series graph is fully covered by a box. The box is divided into four sub-boxes, for example. The number of boxes needed to cover the entire time series is counted. Following the same rule, these sub-boxes are divided into smaller boxes. The different box sizes (α) (also called *scales*) and the number N of validated boxes are recorder. The slope of the curve $\log N(\alpha)$ versus $\log(\alpha)$ gives the fractal dimension.

$$d = \lim_{\alpha \rightarrow 0} \log \frac{N(\alpha)}{\log(\frac{1}{\alpha})} \quad (8)$$

The “Variation estimator” is based on the 2nd order Variogram of a stochastic process as described in (Adler, 1981; Gneiting, Sevcíková, & Percival, 2012). In this case, a fractal dimension is computed for each value of the time lag τ .

ACKNOWLEDGMENTS

This work was supported by the Nappi Family Foundation Research Scholar Project and Lush Prize of Young Researchers in Americas. M.Z. acknowledges support from American Heart Association (AHA) postdoctoral fellowship 16POST27750031. P.H. acknowledges support from the National Science Foundation Integrative Graduate Education and Research Traineeship (NSF IGERT), DMR-DGE-1068780. N.H., B.S., and K.E.H. acknowledge support from NIH-NCATS UH3TR000487 and NIH-NHLBI R01HL130417.

REFERENCES:

- Adler, R. J. (1981). Sample function erraticism and Hausdorff dimension. In *The Geometry of Random Fields* (pp. 184–252). John Wiley and Sons Ltd.
- Ahokas, J. T., Davies, C., & Ravenscroft, P. J. (1984). Comparison of Beta-adrenoceptor antagonists as modulators of drug metabolism: effect of lipophilicity on microsomal phase I and phase II reactions. *British Journal of Clinical Pharmacology*, 17, 103–105.
- Bazan, C., Torres Barba, D., Blomgren, P., & Paolini, P. (2011). Image processing techniques for assessing contractility in isolated neonatal cardiac myocytes. *International Journal of Biomedical Imaging*, 2011. <http://doi.org/10.1155/2011/729732>
- Brzozowska, E., & Borowska, M. (2016). Selection of Phase Space Reconstruction Parameters for EMG Signals of the Uterus. *Studies in Logic, Grammar and Rhetoric*, 47(1), 47–59. <http://doi.org/10.1515/slgr-2016-0046>
- Cîndea, N., Odille, F., Bosser, G., Felblinger, J., & Vuissoz, P. A. (2010). Reconstruction from free-breathing cardiac MRI data using reproducing kernel Hilbert spaces. *Magnetic Resonance in Medicine*, 63(1), 59–67. <http://doi.org/10.1002/mrm.22170>
- Duan, Q., Angelini, E., & Gerard, O. (2006). Cardiac motion analysis based on optical flow on real-time three-dimensional ultrasound data, 2006. Retrieved from <http://academiccommons.columbia.edu/catalog/ac:128460>
- Gao, Z., & Jin, N. (2009). Complex network from time series based on phase space reconstruction. *Chaos*, 19(3). <http://doi.org/10.1063/1.3227736>
- Gneiting, T., Sevcíková, H., & Percival, D. B. (2012). Estimators of Fractal Dimension: Assessing the Roughness of Time Series and Spatial Data. *Statistical Science Donald B. Percival Is Principal*

Mathematician Applied Physics Laboratory, 27(2), 247–277. <http://doi.org/10.1214/11-STS370>

Hassanein, A. S., Khalifa, A. M., Al-Atabany, W., & El-Wakad, M. T. (2014). Performance of Optical Flow tracking approaches for cardiac motion analysis. *Middle East Conference on Biomedical Engineering, MECBME*, 143–146. <http://doi.org/10.1109/MECBME.2014.6783226>

Hossain, M. M., Shimizu, E., Saito, M., Ramachandra Rao, S., Yamaguchi, Y., & Tamiya, E. (2010). Non-invasive characterization of mouse embryonic stem cell derived cardiomyocytes based on the intensity variation in digital beating video. *The Analyst*, 135(7), 1624. <http://doi.org/10.1039/c0an00208a>

Huebsch, N., Loskill, P., Deveshwar, N., Spencer, C. I., Judge, L. M., Mandegar, M. A., ... Conklin, B. R. (2016). Miniaturized iPS-Cell-Derived Cardiac Muscles for Physiologically Relevant Drug Response Analyses. *Scientific Reports*, 6(April), 24726. <http://doi.org/10.1038/srep24726>

Huebsch, N., Loskill, P., Mandegar, M. A., Marks, N. C., Sheehan, A. S., Ma, Z., ... Healy, K. E. (2015). Automated Video-Based Analysis of Contractility and Calcium Flux in Human-Induced Pluripotent Stem Cell-Derived Cardiomyocytes Cultured over Different Spatial Scales. *Tissue Engineering Part C: Methods*, 21(5), 467–479. <http://doi.org/10.1089/ten.tec.2014.0283>

Huffaker, R. (1997). Phase Space Reconstruction from Time Series Data : Where History Meets Theory, 1(c), 1–9.

Kempf, H., Olmer, R., Kropp, C., Rückert, M., Jara-Avaca, M., Robles-Diaz, D., ... Zweigerdt, R. (2014). Controlling expansion and cardiomyogenic differentiation of human pluripotent stem cells in scalable suspension culture. *Stem Cell Reports*, 3(6), 1132–1146. <http://doi.org/10.1016/j.stemcr.2014.09.017>

Kliková, B., & Raidl, A. (2011). Reconstruction of Phase Space of Dynamical Systems Using Method of

Time Delay. *Proceedings of the 20th Annual Conference of Doctoral Students - WDS 2011*, 83–87.

Krakovská, A., Mezeiová, K., & I, H. B. (2015). Use of False Nearest Neighbours for Selecting Variables and Embedding Parameters for State Space Reconstruction, 2015.

Lee, E. K., Kurokawa, Y. K., Tu, R., George, S. C., & Khine, M. (2015). Machine learning plus optical flow: a simple and sensitive method to detect cardioactive drugs. *Scientific Reports*, 5(January), 11817. <http://doi.org/10.1038/srep11817>

Lian, X., Hsiao, C., Wilson, G., Zhu, K., Hazeltine, L. B., Azarin, S. M., ... Palecek, S. P. (2012). Robust cardiomyocyte differentiation from human pluripotent stem cells via temporal modulation of canonical Wnt signaling. *Proceedings of the National Academy of Sciences*, 109(27), E1848–E1857. <http://doi.org/10.1073/pnas.1200250109>

Liang, P., Lan, F., Lee, A. S., Gong, T., Sanchez-Freire, V., Wang, Y., ... Wu, J. C. (2013). Drug screening using a library of human induced pluripotent stem cell-derived cardiomyocytes reveals disease-specific patterns of cardiotoxicity. *Circulation*, 127(16), 1677–1691. <http://doi.org/10.1161/CIRCULATIONAHA.113.001883>

Maddah, M., Heidmann, J. D., Mandegar, M. A., Walker, C. D., Bolouki, S., Conklin, B. R., & Loewke, K. E. (2015). A non-invasive platform for functional characterization of stem-cell-derived cardiomyocytes with applications in cardiotoxicity testing. *Stem Cell Reports*, 4(4), 621–631. <http://doi.org/10.1016/j.stemcr.2015.02.007>

Mathur, A., Loskill, P., Shao, K., Huebsch, N., Hong, S., Marcus, S. G., ... Healy, K. E. (2015). Human iPSC-based cardiac microphysiological system for drug screening applications. *Scientific Reports*, 5, 8883. <http://doi.org/10.1038/srep08883>

Mironyuk, O. Y., & Loskutov, A. Y. (2006). Detection of cardiac pathologies using dimensional

characteristics of RR intervals in electrocardiograms. *Biophysics*, 51(1), 115–119.

<http://doi.org/10.1134/S0006350906010179>

Narayan, S. M., Wright, M., Derval, N., Jadidi, A., Forclaz, A., Nault, I., ... Hocini, M. (2011).

Classifying fractionated electrograms in human atrial fibrillation using monophasic action potentials and activation mapping: Evidence for localized drivers, rate acceleration, and nonlocal signal etiologies. *Heart Rhythm*, 8(2), 244–253. <http://doi.org/10.1016/j.hrthm.2010.10.020>

Navarrete, E. G., Liang, P., Lan, F., Sanchez-Freire, V., Simmons, C., Gong, T., ... Wu, J. C. (2013).

Screening drug-induced arrhythmia events using human induced pluripotent stem cell-derived cardiomyocytes and low-impedance microelectrode arrays. *Circulation*, 128(SUPPL.1).

<http://doi.org/10.1161/CIRCULATIONAHA.112.000570>

Richter, M., & Schreiber, T. (1998). Phase space embedding of electrocardiograms. *Physical Review E*, 58(5), 6392–6398. <http://doi.org/10.1103/PhysRevE.58.6392>

Sinnecker, D., Laugwitz, K. L., & Moretti, A. (2014). Induced pluripotent stem cell-derived

cardiomyocytes for drug development and toxicity testing. *Pharmacology and Therapeutics*, 143(2), 246–252. <http://doi.org/10.1016/j.pharmthera.2014.03.004>

Sklar, J., Johnston, G. D., Overlie, P., Gerber, J. G., Brammell, H. L., Gal, J., & Nies, A. S. (1982). The effects of a cardioselective (metoprolol) and a nonselective (propranolol) beta-adrenergic blocker on the response to dynamic exercise in normal men. *Circulation*, 65(5), 894–899.

<http://doi.org/10.1161/01.CIR.65.5.894>

Takens, F. (1981). Detecting strange attractors in turbulence. *Lecture Notes in Mathematics*, 898, 366–381.

Torkashvand, P., Behnam, H., & Sani, Z. A. (2012). Modified Optical Flow Technique for Cardiac

Motions Analysis.pdf, 2(3).

Wood, M. A., Moskovljevic, P., Stambler, B. S., & Ellenbogen, K. A. (1996). Comparison of bipolar atrial electrogram amplitude in sinus rhythm, atrial fibrillation, and atrial flutter. *PACE - Pacing and Clinical Electrophysiology*, 19(2), 150–156. <http://doi.org/10.1111/j.1540-8159.1996.tb03306.x>

Xu, B., Jacquir, S., Laurent, G., Bilbault, J.-M., & Binczak, S. (2014). Analysis of an experimental model of in vitro cardiac tissue using phase space reconstruction. *Biomedical Signal Processing and Control*, 13, 313–326. <http://doi.org/10.1016/j.bspc.2014.06.005>

Xu, X. Q., Soo, S. Y., Sun, W., & Zweigerdt, R. (2009). Global Expression Profile of Highly Enriched Cardiomyocytes Derived from Human Embryonic Stem Cells. *Stem Cells*, 27(9), 2163–2174. <http://doi.org/10.1002/stem.166>

Yu, Y., Sun, S., Wang, S., Zhang, Q., Li, M., Lan, F., ... Liu, C. (2016). Liensinine- and neferine-induced cardiotoxicity in primary neonatal rat cardiomyocytes and human-induced pluripotent stem cell-derived cardiomyocytes. *International Journal of Molecular Sciences*, 17(2). <http://doi.org/10.3390/ijms17020186>

FIGURE LEGENDS

Figure 1. Process workflow of hiPS-CM contractile motion characterization

The contractile motion of hiPS-CMs was recorded as beating videos, which were analyzed using motion tracking software to generate motion vectors and contractile motion waveforms. This data was then analyzed using PSR to compute the dimensional parameters. The embedding dimension characterizes the regularity of the contractile motions, which reflects the changes in beat rhythm and overall gross motion. The fractal dimension characterizes the complexity, which reflects the secondary aberrations present within each beat cycle.

Figure 2. Reconstruction of cardiac motion waveforms into phase space.

The phase spaces of a regular (a) and a complex (c) cardiac contractile motions are plotted along with their corresponding motion waveforms (b, d). The embedding dimensions from a single motion waveform were computed from PSR to compare the differences in regularity between two contractile motions (e). The regularity dimensions derived the embedding dimensions were plotted with respect to τ (f). The average fractal dimension across all τ was computed from PSR (g) and then plotted with respect to τ (h)

Figure 3. Motion waveform decomposition along X and Y directions.

A motion waveform (total) was decomposed into X and Y components (a), and corresponding phase spaces were reconstructed respectively (b). Embedding and regularity dimensions of X-axis and Y-axis motions showed no significant differences compared to the total motion (c, d), while fractal dimension of Y-axis motion was significantly lower than the X-axis and total motion (e, f).

Figure 4. PSR analysis of secondary system aberrations.

A motion waveform was supplied with random noise ranging from 2.5%-50% (a), and corresponding phase space was reconstructed to compute the dimensional parameters respectively for different degrees of noise. No significant difference was found based on embedding and regularity dimensions among the contractile motions with different noise level (b, c), but fractal dimensions exhibited significant increase with the increase of the noise level (d, e).

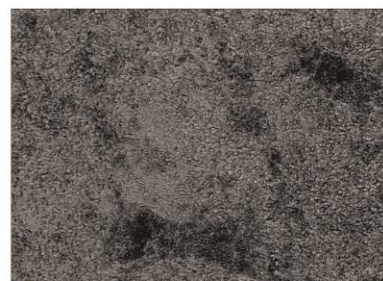
Figure 5. PSR analysis of drug-induced arrhythmic contractile motions.

(a) The application of propranolol to hiPS-CMs increased the average embedding dimension with the increase of drug concentrations, which correlated to a reduction in regularity dimension. No significant difference was found for fractal dimension between baseline control and drug exposure. (b) E4031 induced significant increases in the embedding and regularity dimensions between controls and drug exposure. High dosage of E4031 (100 nM) induced a significant increase of fractal dimension on the hiPS-CMs in comparison to the control and low dosage. (c) PSR analysis showed that treatment of hiPS-CM with metoprolol has no significant influence on the embedding, regularity and fractal dimensions. (d) Low dosage of isoproterenol (50 nM) decreased the embedding dimension, which corresponded to a rise in the regularity of the system. In contrast, high dosage of isoproterenol (10 μ M) increased the embedding and fractal dimensions, indicating the contractile motions of hiPS-CMs gained aberrations but lost regularity.

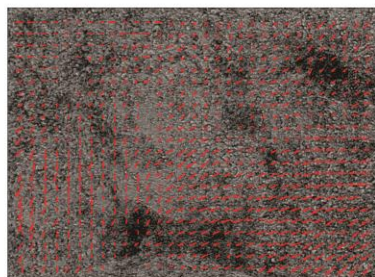
Figure 6. Drug-induced arrhythmia comparison of motion tracking versus calcium flux.

Brightfield and fluorescence videos of drug-treated GCaMP6f hiPSC-CMs were recorded for (a) motion tracking analysis and (b) calcium flux analysis. (c) Waveforms generated from each assay were subjected to PSR analysis. PSR analysis of both methods illustrated the sensitivities to drug interference by

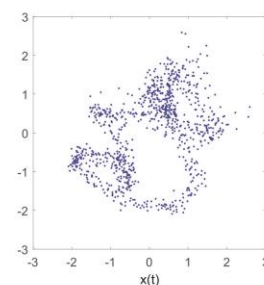
quantifying changes in the embedding and fractal dimensions as a result of (d) isoproterenol and (e) propranolol induced-arrhythmias. All scale bars are 100 μm .



Motion
tracking
analysis



Phase space
reconstruction
of contraction
motion



PSR output parameters

